Materials Science and Engineering C 49 (2015) 579–587

Contents lists available at ScienceDirect

Materials Science and Engineering C

journal homepage: www.elsevier.com/locate/msec

A sensitive glucose biosensor based on Ag@C core–shell matrix

Xuan Zhou [a], Xingxin Dai [a], Jianguo Li [a], Yumei Long [a,b,*], Weifeng Li [a,**], Yifeng Tu [a,b]

[a] College of Chemistry, Chemical engineering and Materials Science, Soochow University, Suzhou, Jiangsu 215123, PR China
[b] The Key Lab of Health Chemistry and Molecular Diagnosis of Suzhou, PR China

ARTICLE INFO

Article history:
Received 30 October 2014
Received in revised form 30 December 2014
Accepted 17 January 2015
Available online 19 January 2015

Keywords:
Ag@C core–shell structure
Glucose oxidase
Biosensor
Electrochemistry

ABSTRACT

Nano-Ag particles were coated with colloidal carbon (Ag@C) to improve its biocompatibility and chemical stability for the preparation of biosensor. The core–shell structure was evidenced by transmission electron microscope (TEM) and the Fourier transfer infrared (FTIR) spectra revealed that the carbon shell is rich of function groups such as —OH and —COOH. The as-prepared Ag@C core–shell structure can offer favorable microenvironment for immobilizing glucose oxidase and the direct electrochemistry process of glucose oxidase (GOD) at Ag@C modified glassy carbon electrode (GCE) was realized. The modified electrode exhibited good response to glucose. Under optimum experimental conditions the biosensor linearly responded to glucose concentration in the range of 0.05–2.5 mM, with a detection limit of 0.02 mM (S/N = 3). The apparent Michaelis–Menten constant (K_M^{app}) of the biosensor is calculated to be 1.7 mM, suggesting high enzymatic activity and affinity toward glucose. In addition, the GOD-Ag@C/Nafion/GCE shows good reproducibility and long-term stability. These results suggested that core–shell structured Ag@C is an ideal matrix for the immobilization of the redox enzymes and further the construction of the sensitive enzyme biosensor.

1. Introduction

Accurate and tight blood glucose monitoring is crucial to the diagnosis and management of diabetes, which is one of the worldwide public health problems [1]. For this reason, many methods have been developed to determine glucose. Among these, electrochemical method based on immobilization of GOD plays a leading role because of its simplicity, selectivity and high sensitivity. GOD is a homodimer containing two tightly bound flavin adenine dinucleotide (FAD) redox centers that can catalyze the electron transfer from glucose to gluconolactone. Unfortunately, direct electron transfer between GOD and the electrode is extremely difficult due to its deeply embedded FAD within a protective protein shell or its denaturation upon adsorption onto the surface of the electrode. Therefore, it is a major challenge to develop desirable matrix for immobilizing GOD onto the transducer surface, which should provide a desirable microenvironment between the redox sites of GOD and the electrode surface.

It has been well established that nanomaterials are favorable for enzymatic immobilization due to their unique microstructures and properties at nanometer size scale, and hence have attracted much interest in the field of electrochemical biosensor [2–11]. Metal nanoparticles, for example, have found extensive application in glucose biosensors by enhancing surface area and contributing to electron transfer from enzyme to electrode, which subsequently led to improvements in detection signal [12]. However, metal nanoparticles usually have relatively inert surfaces and/or unsatisfactory biocompatibility, which make surface modification almost unavoidable before use as supports or templates [13–15]. For example, porous carbon stabilized gold nanoparticles have recently been reported for their good biocompatibility and catalytic property [16,17].

Recently, core–shell hetero-nanostructure has attracted significant attention for its applications in many fields including biomedical, electronics, optical, and catalysis [18,19]. Such hybrid structures can possess multifunctional properties, which can be adjusted by changing either the constituting materials or the core to shell ratio [20]. Therefore, many attempts have been made to achieve core–shell structures with controlled shell chemistry. Carbon coating is one of the most attractive shell layers for its low preparation cost, chemical activity, and biocompatibility [21–23]. Moreover, rich functional groups in the as-formed colloidal carbon shell are much helpful to the loading of other functional molecules for further bioassay applications [24,25].

Silver has the highest electrical conductivity among all metals and is probably the most important material in plasmonics. However, Ag nanostructures are considered to be toxic and unstable [26]. The problem can be solved by applying a biocompatible coating to eliminate the reactivity and toxicity of nano-Ag [27,28]. In the present work, nano-Ag particles coated by colloidal carbon shell were synthesized through a hydrothermal process and the resulting core–shell structure was employed to immobilize GOD for the construction of the glucose biosensor. The colloidal carbon shell of Ag@C provided a biocompatible microenvironment for GOD to keep its bioactivity and was also acting as

* Correspondence to: Y. Long, College of Chemistry, Chemical engineering and Materials Science, Soochow University, Suzhou, Jiangsu 215123, PR China.
** Corresponding author.
E-mail addresses: yumeilong@suda.edu.cn (Y. Long), liweifeng@suda.edu.cn (W. Li).

http://dx.doi.org/10.1016/j.msec.2015.01.063
0928-4931/

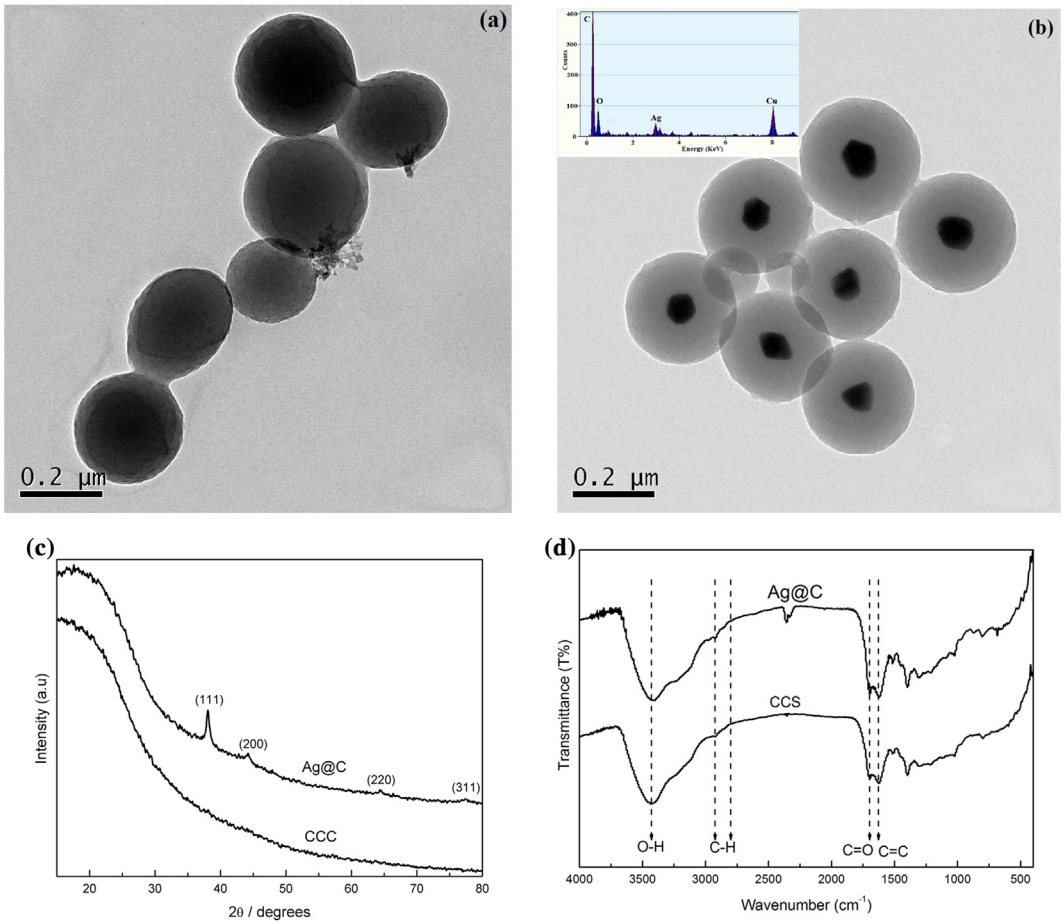

Fig. 1. TEM images of colloidal carbon sphere (a) and Ag@C core–shell structure (b), inset is the EDS of Ag@C; XRD pattern (c) and FTIR (d) of Ag@C.

support matrix to strengthen the immobilization layer via functional groups. In addition, nano-Ag core can facilitate the direct electron transfer between redox centers of GOD and electrode surface. The direct electrochemical behaviors of GOD on the Ag@C (denoted as GOD-Ag@C/GC electrode) were investigated and the obtained biosensor exhibited good electrocatalysis toward glucose.

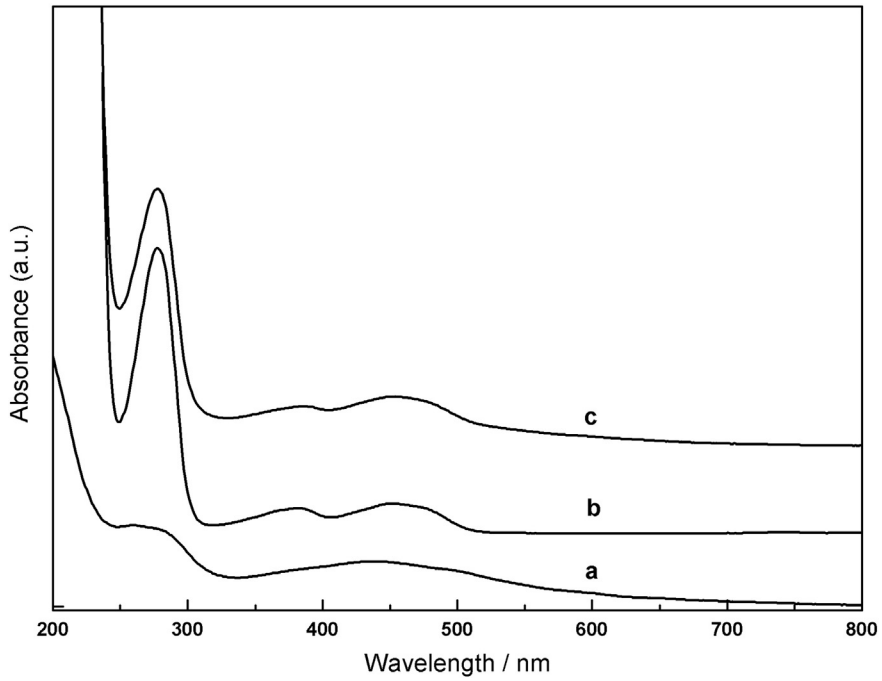

Fig. 2. UV–vis absorption spectra of the Ag@C (a), native GOD (b) and GOD-Ag@C (curve c).

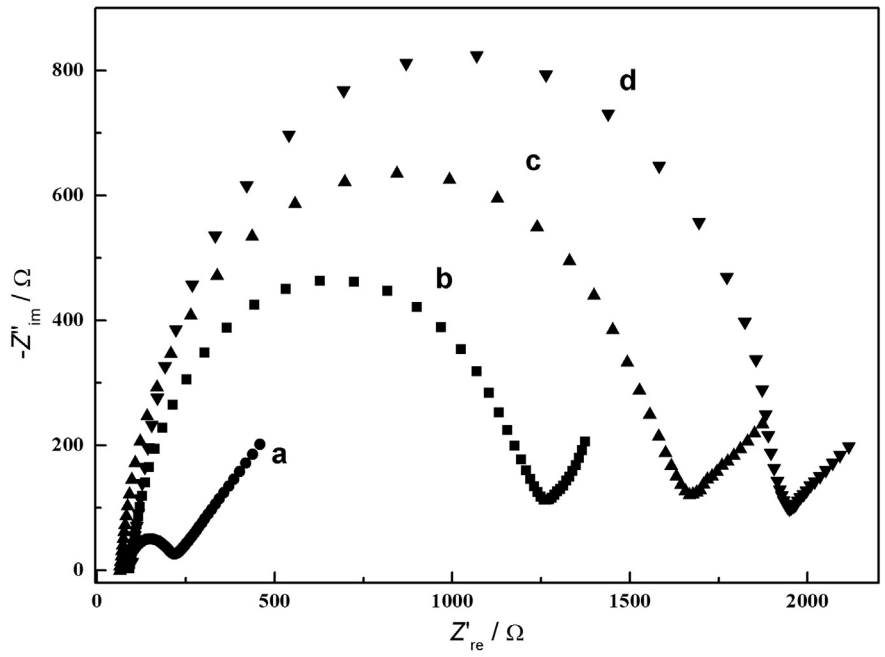

Fig. 3. Electrochemical impedance spectra of bare GCE (a), Ag@C/Nafion/GCE (b), GOD-Ag@C/Nafion/GCE (c) and GOD/Nafion/GCE (d) measured in 0.1 M KCl containing 2.5 mM $K_3[Fe(CN)_6]/K_4[Fe(CN)_6]$ mixture.

2. Experimental

2.1. Chemicals

GOD (EC 1.1.3.4, 108 U/mg, from *Aspergillus niger*) and Nafion (5 wt.% solution) were purchased from Sigma and used without further purification. β-D-(+)-Glucose, $AgNO_3$, NaH_2PO_4 and Na_2HPO_4 were obtained from Sinopharm Chemical Reagent Co. Ltd. The stock GOD solution was prepared in the 0.1 M phosphate buffer solution (PBS, pH 7.0) and stored at 4 °C. The 0.1 M PBS at various pH values was prepared by mixing the stock solutions of 0.1 M NaH_2PO_4 and 0.1 M Na_2HPO_4 with different proportions. All other chemicals were of analytical grade and were prepared with doubly distilled water.

2.2. Apparatus

The obtained products were characterized by TEM, energy-dispersive X-ray spectroscopy (EDS) (FEI Tecnai G20, an acceleration voltage of 200 kV), FTIR spectroscopy (Prostar LC240) and UV–vis optical absorbance spectra (TU-1810, Beijing, China).

Electrochemical measurements were performed on a CHI611D electrochemical workstation (Chenhua Instruments Co., Shanghai, China).

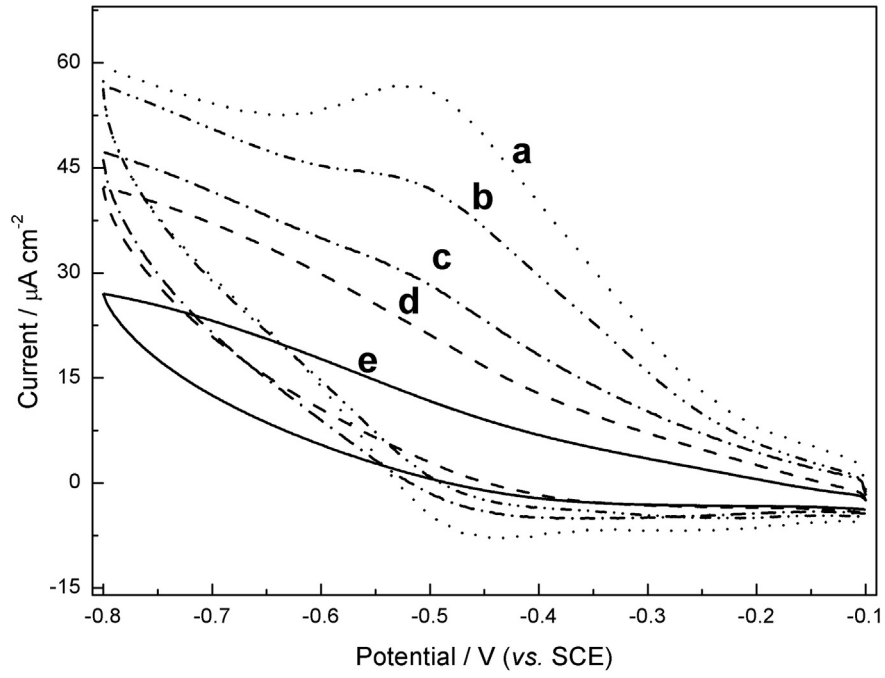

Fig. 4. Cyclic voltammograms for the GOD-Ag@C/Nafion/GCE (a), GOD-CCS/Nafion/GCE (b), GOD/Nafion/GCE (c), Ag@C/Nafion/GCE (d) and the bare GCE (e) in N_2-saturated PBS (0.1 M and pH 7.0) at a scan rate of 0.1 V/s.

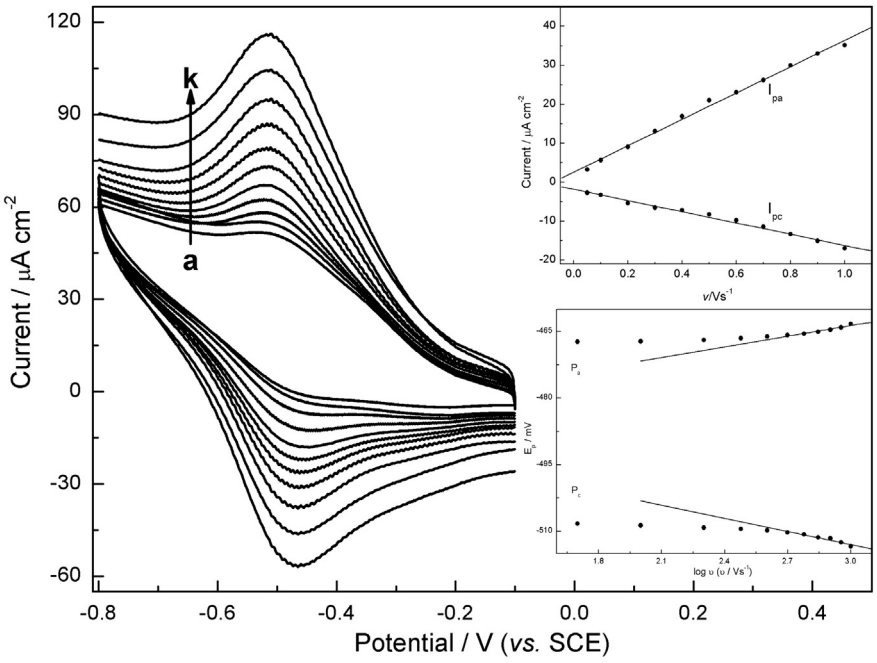

Fig. 5. Cyclic voltammograms of the GOD-Ag@C/Nafion/GCE in N_2-saturated 0.1 M PBS (pH 7.0) at various scan rates (from inner to outer: 0.05, 0.1, 0.2, 0.3, 0.4, 0.5, 0.6, 0.7, 0.8, 0.9 and 1.0 V s^{-1}). Inset up: plots of the anodic and cathodic peak currents versus potential scan rates; Inset down: anodic and cathodic peak potentials vs. log υ.

The measurements were based on a conventional three-electrode system, which includes the GOD-Ag@C/Nafion/GCE electrode as working electrode, a platinum electrode as auxiliary electrode, and a saturated calomel electrode (SCE) as reference electrode, respectively. Electrochemical impedance spectroscopy (EIS) was performed on a RST5200 electrochemical workstation (Suzhou Risetest Instrument Co. Ltd., China) in a background solution of 0.1 M KCl containing 1.0×10^{-3} M $[Fe(CN)_6]^{3-/4-}$. All measurements were performed at room temperature (25 ± 2 °C).

2.3. Synthesis of Ag@C core–shell composites

Ag@C core–shell composites were synthesized according to one-pot hydrothermal method uncovered in a previous report [24]. Briefly, 2 mL 0.03 M $AgNO_3$ was slowly dropped into 0.5 M glucose solution (38 mL) under vigorous stirring. After finishing the addition of $AgNO_3$ solution, the resulting solution was transferred into a Teflon-lined autoclave (50 mL in volume) and then maintained at 180 °C for 4 h. After the

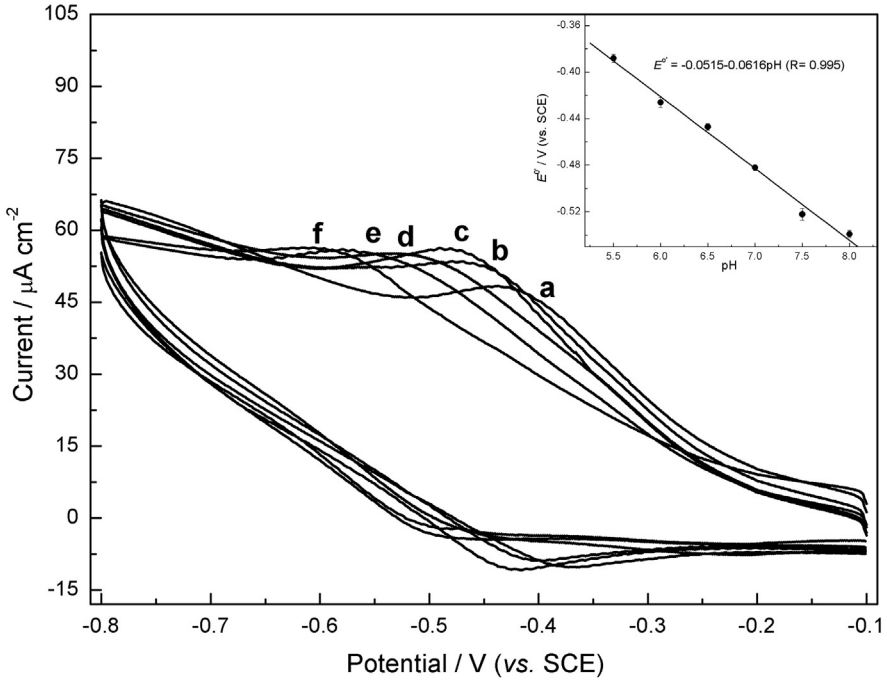

Fig. 6. Cyclic voltammograms of the GOD-Ag@C/Nafion/GCE in N_2-saturated 0.1 M PBS (pH 7.0) at different pHs (a—5.5, b—6.0, c—6.5, d—7.0, e—7.5 and f—8.0). Inset: formal potentials as a function of pH at a scan rate of 0.1 V/s.

cooling of the autoclave, Ag@C composite was collected by centrifugation and washed with water and ethanol several times. Finally, the as-synthesized products were dried at 60 °C overnight. For comparison, colloidal carbon sphere (CCS) was prepared following a similar procedure free of $AgNO_3$.

2.4. Preparation of the GOD-Ag@C/Nafion/GCE

Prior to modification, GCEs (diameter 3 mm) were carefully polished with 1.0 μm, 0.3 μm and 0.05 μm alumina slurries in sequence and then rinsed ultrasonically with doubly distilled water. After sonicating in absolute ethanol and water, respectively, the cleaned GCEs were dried with nitrogen. Enzyme electrode was fabricated by a simple casting method. Firstly, an Ag@C suspension (2 mg/mL) was obtained by dispersing appropriate amount of Ag@C into water and sonicating for 30 min until a homogeneous sol was obtained. GOD solution with a concentration of 10 mg/mL was prepared in PBS (0.1 M, pH 7.0). Then, enzyme immobilization was achieved by mixing GOD solution and Ag@C suspension at volume ratio of 2:1, followed by ultrasonic treatment and stored at 4 °C for 24 h for GOD adsorption. Finally, 15 μL of the GOD-Ag@C mixture was spread onto the surface of GCE and dried in refrigerator at 4 °C. After 3.0 μL of 1% Nafion

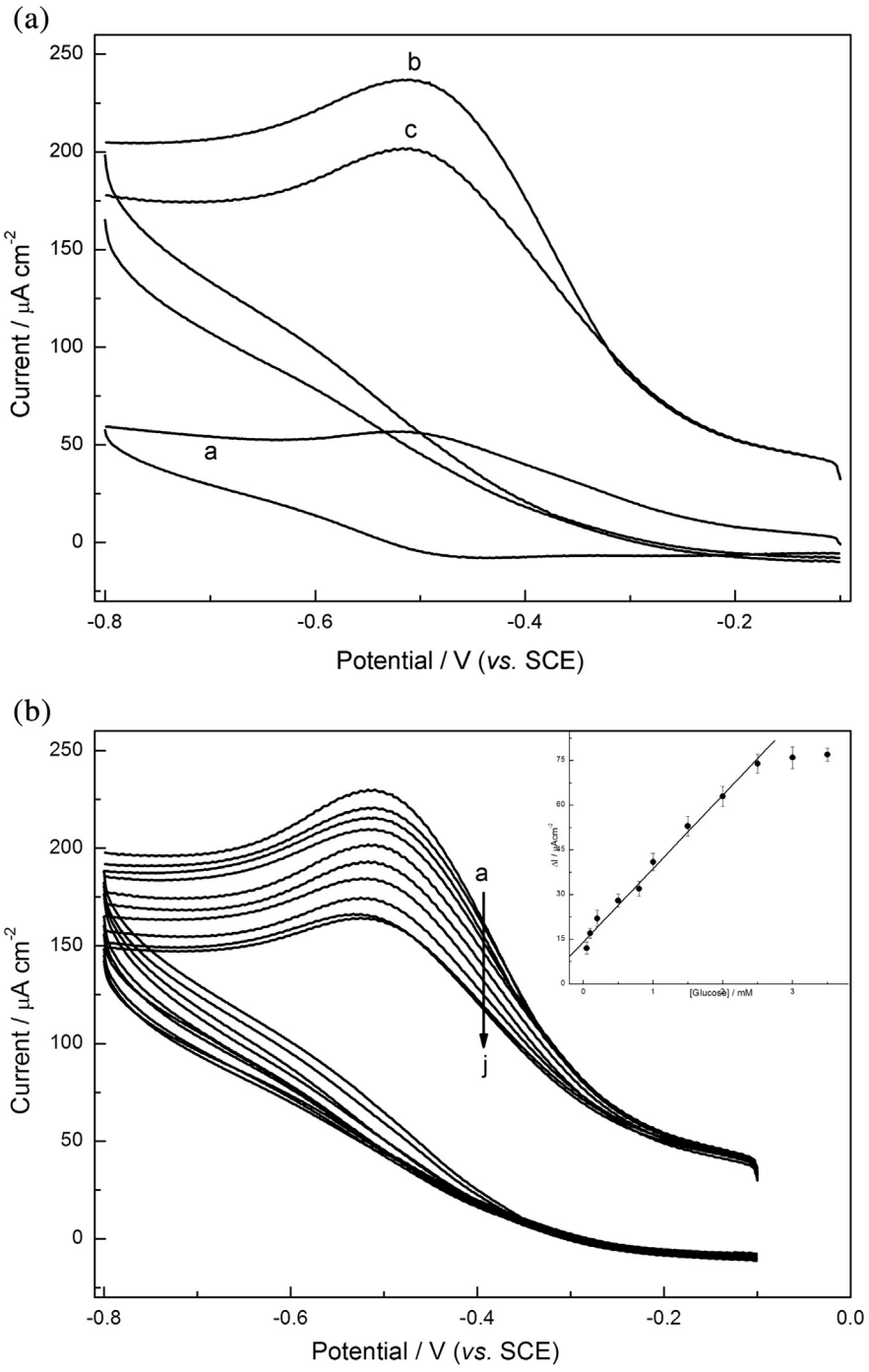

Fig. 7. (A) Cyclic voltammograms of the GOD-Ag@C/Nafion/GCE in N_2-saturated (a), air-saturated 0.1 M PBS (pH 7.0) without (b) and with (c) 1 mM glucose at the scan rate of 0.1 V/s; (B) cyclic voltammograms of the GOD-Ag@C/Nafion/GCE in air-saturated 0.1 M PBS including 0.05, 0.1, 0.2, 0.5, 0.8, 1.0, 1.5, 2.0, 2.5 and 3.0 mM glucose (from a to j) at a scan rate of 0.1 V/s. Inset: Dependence of the decreased reduction peak current of the GOD-Ag@C/Nafion/GCE on the concentration of glucose.

solution was dropped on the GOD-Ag@C modified electrode surface, the GOD-Ag@C/Nafion/GCE was obtained. In control experiment, the GOD-CCS/Nafion/GCE was also fabricated following the same process.

3. Results and discussion

3.1. Characterization of Ag@C composites

TEM images of the CCS (Fig. 1a) and Ag@C (Fig. 1b) samples show that they were spherical and monodisperse with a particle size of 200–300 nm. In the case of Ag@C sample, each of particles consists of Ag core with diameters in the range of 40–60 nm and carbon shell with thickness about 100 nm. The EDS spectrum shown in the inset of Fig. 1b gives direct evidence of the existence of Ag and C elements, and the signals of Cu element originate from TEM copper grid. In addition, oxygen EDS signal can be observed in the EDS spectrum, which is ascribed to functional group in the carbon shell. Fig. 1c shows the XRD patterns of CCS and Ag@C samples. The sharp diffraction peaks in the 2θ range of 35–80° confirmed the existence of face-centered cubic Ag (JCPDS 87-0597) phase, while the broad peak in the 2θ range of 15–35° should be assigned to the amorphous carbon shell. The functional groups of surface of the sample are investigated by FTIR, as shown in Fig. 1d. The FTIR spectra clearly identify the functional groups. The signature peaks at about 1710 and 1620 cm^{-1} correspond to C═O and C═C vibrations, respectively. The absorption band ranging from 1000 cm^{-1} to 1300 cm^{-1} is ascribed to the C–OH stretching and OH bending vibrations, which suggests the existence of large numbers of residual hydroxyl groups. Partially dehydrated residues improve the hydrophilicity and stability of the Ag@C in aqueous systems, and greatly extend their applications in biochemistry, diagnostics, and drug delivery. Furthermore, these functional groups outside can enhance the immobility of the Ag@C composites on the GCE and improve the absorption to the polar molecules.

The conformational integrity of GOD attached on Ag@C composites is investigated by UV–vis spectroscopy. Fig. 2 shows the UV–vis absorption spectra of the Ag@C (curve a), native GOD (curve b) and GOD-Ag@C bio-composite (curve c). For the native GOD, there are three characteristic absorption bands, in which the absorption band centered at 277 nm should be assigned to the characteristic of polypeptide chains, and the other two weak absorption bands peaking at 380 nm and 458 nm are caused by the oxidized form of flavin group in protein structure [29]. It is interested that the GOD-Ag@C hybrid exhibits the similar optical absorption properties to that of native GOD, suggesting that Ag@C composites have good biocompatibility and do not induce significant denaturation of the GOD.

The EIS is an effective tool to investigate the interfacial properties of the modified electrodes. In the Nyquist plots ($-Z''_{im}$ vs. Z'_{re}), the semicircle portion at higher frequencies corresponds to the electron-transfer limited process and the linear portion at lower frequencies is related with the diffusion process. The electron transfer resistance (R_{et}) can be estimated from the diameter of a semicircle and its value reveals the electron transfer kinetics of the redox electrochemical probe at the electrode interface [30]. Fig. 3 shows the results of EIS measurements performed on the bare and modified GCEs in 0.1 M KCl containing 2.5 mM $K_3[Fe(CN)_6]/K_4[Fe(CN)_6]$ mixture. The R_{et} value of the Ag@C/Nafion/GCE (1170 Ω, curve b) is much larger than that of the bare GCE (127 Ω, curve a), indicating the formation of Ag@C film on the electrode surface and the hindrance effect on the redox couples due to the insulating carbon shell. When the GOD has been immobilized on the Ag@C/Nafion matrix, the R_{et} increases to 1584 Ω (curve c), confirming the successful immobilization of GOD. However, the R_{et} of the GOD-Ag@C/nafion/GCE is smaller than that of the GOD/Nafion/GCE (1861 Ω, curve d), which could be resulted from the larger surface area of GOD-Ag@C/nafion/GCE than that of GOD/Nafion/GCE.

3.2. Direct voltammetry of GOD-Ag@C modified GCE

Fig. 4 shows the cyclic voltammograms (CVs) of different films modified GCEs in PBS (0.1 M and pH 7.0) saturated with N_2 at a scan rate of 0.1 Vs^{-1}. A pair of well-defined redox peaks is observed at the GOD-Ag@C/Nafion/GCE. The formal potential value ($E^{0\prime}$) calculated by averaging the cathodic and anodic peak potentials is −0.488 V (vs. SCE) and the peak-to-peak separation (ΔE_p) is about 42 mV (curve a), which is smaller than that of GOD/graphene–chitosan/GCE [31] and GOD/Au/carbon paste electrode [32]. On the other hand, no redox peak can be found at Ag@C/Nafion/GCE (curve d) and bare GCE (curve e). The results indicated that the redox peaks should be ascribed only to GOD. Thus, a direct electron transfer of GOD in Ag@C/Nafion film has been successfully achieved. In addition, control experiments were conducted at GOD-CCS/Nafion/GCE (curve b) and GOD/Nafion/GCE (curve c), which show a weak electrochemical reaction for the GOD. The above experimental results demonstrated that Ag@C core–shell structure plays an important role in facilitating the direct electron transfer process between the GOD and electrode substrate.

Fig. 5 displays the cyclic voltammograms obtained at GOD-Ag@C/Nafion/GCE in N_2-saturated 0.1 M PBS (pH 7.0) at different scan rates. The peak currents (I_{pa} and I_{pc}) increase with an increasing scan rate. Inset (up) of Fig. 5 illustrates a linear relationship between peak current and scan rate in the range of 50 to 1000 mV/s, and the linear regression equations for the redox process can be expressed as: $I_{pa} = 2.59 + 33.85\upsilon$ (R = 0.998) for anodic peak and $I_{pc} = -1.77–14.43\upsilon$ (R = 0.994) for cathodic peak, respectively. Thus, the GOD redox process occurring at GOD-Ag@C/Nafion/GCE is surface-confined. In the case of surface-controlled electrochemical process, the electron transfer rate constant (k_s) can be estimated using Laviron's equation [33]. Inset (down) of Fig. 5 is the plot of anodic and cathodic peak potentials vs. log υ. Thereby, the charge-transfer coefficient and the apparent electron transfer rate constant (k_s) of GOD at GOD-Ag@C/Nafion/GCE are estimated to be 0.45 and 2.01 s^{-1}, respectively. This further suggests the fast electron transfer kinetics process in the presence of Ag@C.

The effect of pH on the electrochemical behaviors of the GOD-Ag@C/Nafion/GCE was investigated. As shown in Fig. 6, both anodic and cathodic peak potentials of GOD shift negatively with the increment of the solution pH value. The formal potential ($E^{0\prime}$) versus pH gives a straight line in the range of 5.5–8.0 and the linear regression equation is $E^{0\prime} = -0.0515–0.0616$ pH (R = 0.995) with the slope of −61.6 mV/pH (inset of Fig. 6), which is close to the theoretical value of −58.6 mV/pH for a reversible two-proton/two-electron transfer electrochemical process [34].

Table 1
Comparison of the GOD-Ag@C/Nafion/GCE and other electrodes for glucose determination RGO: reduced graphene oxide; GOx: glucose oxidase; GOD: glucose oxidase; CNx-MWNTs: nitrogen-doped carbon nanotubes; TCS: tetragonal columnar-shaped; CS: chitosan; ERGO: electrochemically reduced grapheme oxide; TU: thiourea; GNSs: graphite nanosheets; G-CdS: graphene-CdS.

Electrode	Linear range (mM)	Detection limit (μM)	Sensitivity ($\mu AmM^{-1} cm^{-2}$)	Ref.
GCE/RGO-GOx	0.1–27	–	1.85	[3]
GOD/CNx-MWNTs/Nafion/GC	0.016–1.02	10	13	[34]
GOx/TCS-TiO_2/chitosan/GCE	0.005–1.32	2	23.2	[37]
CS-GOD-ERGO/GCE	0.02–3.2	1.7	6.82	[38]
GOx-TU/GCE	0.05–5.5	6	5.73	[39]
RGO/Ag/GOD/GCE	0.5–12.5	160	3.84	[40]
GOD-In_2O_3-Chitosan/GCE	0.005–1.3	1.9	7.3	[41]
Nafion-GOD-GNSs	0.2–1.4	–	3.4	[42]
G-CdS-GOD/GCE	2–16	700	1.76	[43]
GOD-Ag@C/Nafion/GCE	0.05–2.5	20	24.65	Here

3.3. Detection of glucose using GOD-Ag@C/Nafion/GCE

The bioactivity of immobilized GOD in GOD-Ag@C/Nafion/GCE was studied by observing the reaction with oxygen since glucose oxidase has electrocatalytic activity to oxygen [35]. Fig. 7a shows the CVs of the GOD-Ag@C/Nafion/GCE in N_2-saturated, air-saturated 0.1 M PBS and air-saturated PBS containing 1 mM glucose at a scan rate of 0.1 V/s. Compared to the peak currents in the N_2-saturated solution (curve a), a significant increase of cathodic peak current and simultaneous decrease

Table 2
Determination of glucose in serum sample using GOD-Ag@C/Nafion/GCE.

Sample	Sample Found* (mM)	Added (mM)	Found (mM)	RSD (%) (n = 5)	Recovery (%)
1	0.43	0.1	0.51	3.6	96.2
2	0.43	0.2	0.66	3.2	104.8
3	0.43	0.3	0.75	2.7	102.7

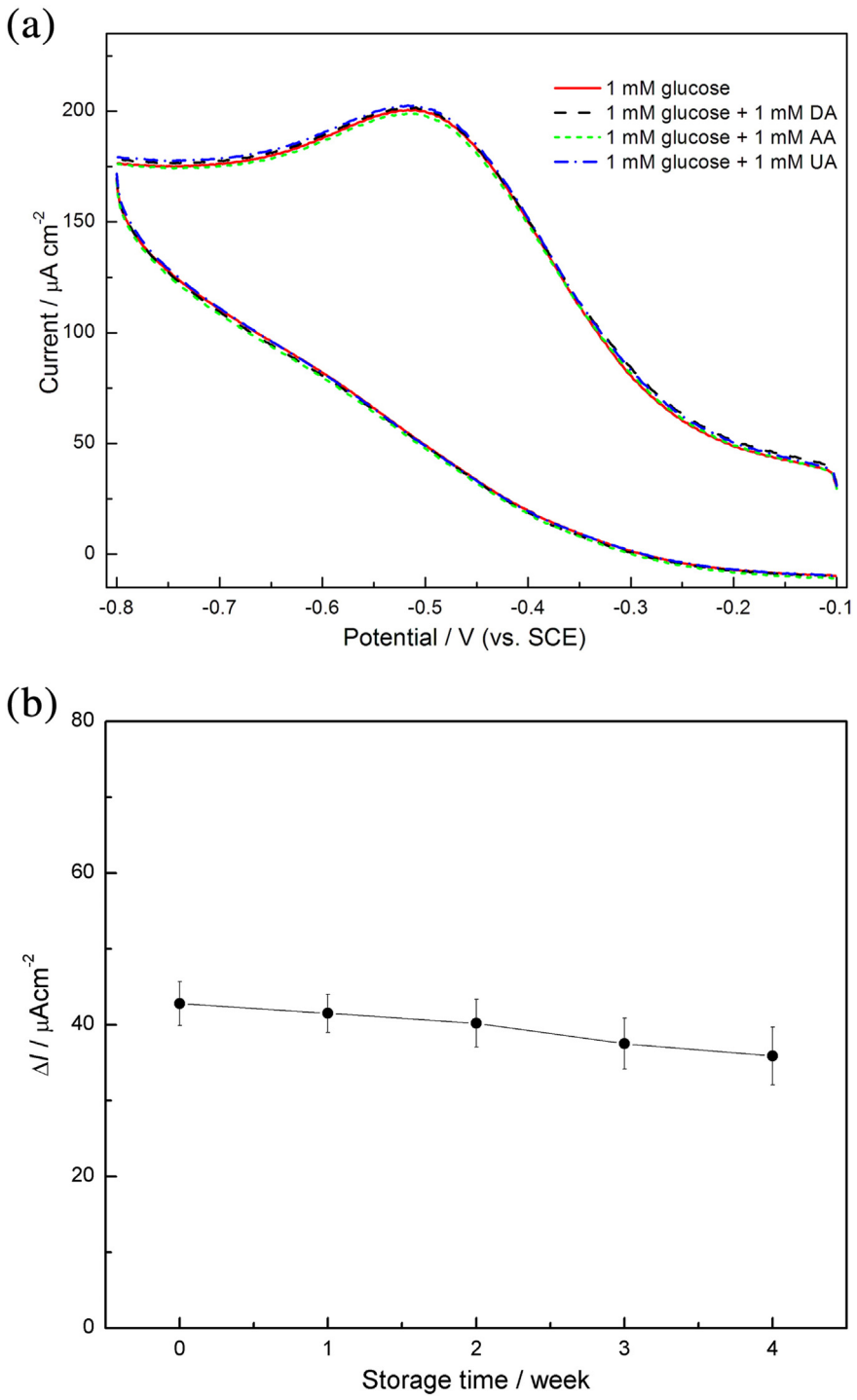

Fig. 8. (A) Cyclic voltammograms of GOD-Ag@C/Nafion/GCE in air-saturated 0.1 M PBS (pH 7.0) containing glucose, glucose + dopamine (DA), glucose + ascorbic acid (AA) and glucose + uric acid (UA), respectively. Scan rate: 0.1 V s^{-1}; (B) the current response of GOD-Ag@C/Nafion/GCE to 1 mM glucose after four weeks of storage at 4 °C in the refrigerator.

of anodic peak current occur in the air-saturated solution (curve b). The redox reactions are expressed as Eqs. (1) and (2).

$$\text{GOD-FAD} + 2e^- + 2H^+ \leftrightarrow \text{GOD-FADH}_2 \quad (1)$$

$$\text{GOD-FADH}_2 + O_2 \rightarrow \text{GOD-FAD} + H_2O_2 \quad (2)$$

It should be noted that the reduction current decreased at the GOD-Ag@C/Nafion/GCE with the introduction of glucose into air-saturated PBS (curve c). The mechanism can be explained as follows:

$$\text{Glucose} + \text{GOD-FAD} \rightarrow \text{GOD-FADH}_2 + \text{gluconolactone}. \quad (3)$$

According to Eq. (3), GOD could catalyze the oxidation of glucose in the presence of oxygen, which would consume oxygen and decrease the concentration of oxygen in the solution. Thus, the addition of glucose would result in the decrease of electrocatalytic reduction current of oxygen, as expressed in Eqs. (1) and (2).

Fig. 7b shows cyclic voltammograms of the GOD-Ag@C modified GCE in air-saturated 0.1 M PBS containing different concentrations of glucose. The cathodic peak currents at the GOD-Ag@C/Nafion/GCE gradually decrease with the increase of the concentration of glucose resulting from the consumption of oxygen. Moreover, the decreased reduction peak currents at the GOD-Ag@C/Nafion/GCE change linearly with the increase of glucose concentration, as shown in the inset of Fig. 7b. Thereby, a glucose biosensor has been developed. The linear response range of the biosensor to glucose concentration is from 0.05 to 2.5 mM with a correlation coefficient of 0.995. The detection limit is 0.02 mM at signal-to-noise of 3 and the sensitivity is calculated to be 24.65 $\mu A mM^{-1}\ cm^{-2}$. In addition, the Michaelis–Menten constant ($K^{app}{}_M$), which reflects biological activity of an immobilized enzyme and the ratio of microscopic kinetic constant, is estimated to be 1.7 mM according to the Lineweaver–Burk equation [36]. The small $K^{app}{}_M$ value indicates that the GOD immobilized on the Ag@C materials has good bioactivity and high affinity to glucose.

The further comparison of GOD-Ag@C/Nafion/GCE with those recent reports of glucose electrochemical sensor is shown in Table 1. As it can be seen, the proposed biosensor exhibited higher sensitivity and a wider linear range than most of them. Moreover, the construction procedure of GOD-Ag@C/Nafion/GCE is simple, environment-friendly, and economical.

3.4. Selectivity, stability and reproducibility of the GOD-Ag@C/Nafion/GCE

The selectivity of the electrode is one of the most important factors for the practical use. In the blood, dopamine (DA), ascorbic acid (AA) and uric acid (UA) are usually coexisted with glucose and might affect the electrochemical response for glucose determination. Therefore, the effect of those interferents on the glucose response was investigated by cyclic voltammograms and the results were given in Fig. 8a. When 1.0 mM DA, AA or UA was added into 1 mM glucose solution (air-saturated 0.1 M PBS, pH 7.0), respectively, no obvious interference can be found to the cathodic current of glucose. These results indicated that the GOD-Ag@C/Nafion/GCE has favorable selectivity.

The stability of the biosensor was investigated. The response current of the GOD-Ag@C/Nafion/GCE in 1 mM glucose solution (air-saturated 0.1 M PBS, pH 7.0) was examined at intervals over a week, as shown in Fig. 8b. After four weeks storage at 4 °C in refrigerator, the biosensor exhibited 14.5% loss as compared to the initial response. The operational stability of the modified electrode was investigated by examining the cyclic voltammetric peak currents of 1 mM glucose and the relative standard deviation was 2.1% for ten successive determinations. Meanwhile, the reproducibility was studied via testing five enzyme electrodes prepared in the same way. The RSD was 5.7% for the determination of 1 mM glucose. These results showed that the GOD-Ag@C/Nafion/GCE possesses good stability and reproducibility. The excellent sensing property of GOD-Ag@C/Nafion/GCE is ascribed to the synergistic effect of carbon shell and nano-Ag core in the Ag@C: Firstly, the biocompatibility of carbon shell can provide a desirable microenvironment for the GOD, allowing it to retain its stability and bioactivity; Secondly, rich functional groups in the carbon shell are favorable to the attachment of GOD, for example, GOD anchor on the Ag@C core–shell matrix through amidation condensation reaction between $-NH_2$ of GOD and –COOH of Ag@C, and hence prevent the leaking of enzyme from the electrode during the repeated applications; Finally, the nano-Ag core has excellent conductivity and electrocatalytic activity.

3.5. Determination of glucose in real serum sample

The feasibility of the GOD-Ag@C/Nafion/GCE in real sample assay was demonstrated by determining glucose in human serum utilizing standard addition method. The serum sample was provided by a local hospital without any sample pretreatment and the original glucose concentration in the serum was determined to be 4.3 mM. Typically, 1 mL plasma sample was added into 9 mL 0.1 M PBS (pH 7.0) saturated with air and then 20 μL 50 mM glucose was added into the system for standard addition measurement. The corresponding results were shown in Table 2. A small relative standard deviation (RSD) values (less than 3.6%) and high recovery values (96.2–104.8%) revealed that the proposed biosensor is reliable and effective.

4. Conclusions

In this work, core–shell structured Ag@C particles were synthesized and employed for the immobilization of GOD. The combination of Ag core and carbon shell can provide a biocompatible microenvironment for GOD and facilitate the electron transfer between GOD and electrode, thus improving its affinity and sensitivity for glucose. The as-prepared biosensor possesses excellent properties, such as good stability and reproducibility, high sensitivity, a low detection limit and a wide linear detection range. Moreover, the proposed biosensor was successfully applied in real sample assay and satisfactory results were obtained. The strategy in this work demonstrated the advantages of core–shell structured materials like Ag@C in the fabrication of biosensors and provides a new way for developing high-performance bio-molecule biosensors.

Acknowledgments

This work was supported by the National Natural Science Foundation of China (21005053), the Priority Academic Program Development of Jiangsu Higher Education Institutions and the Project of Scientific and Technologic Infrastructure of Suzhou (SZS201207).

References

[1] R.R. Banerjee, S.M. Rangwala, J.S. Shapiro, A.S. Rich, B. Rhoades, Y. Qi, J. Wang, M.W. Rajala, A. Pocai, P.E. Scherer, C.M. Steppan, R.S. Ahima, S. Obici, L. Rossetti, M.A. Lazar, Regulation of fasted blood glucose by resistin, Science 303 (2004) 1195–1198.
[2] W.B. Zhao, Y. Fang, Q.S. Zhu, K. Wang, M. Liu, X.H. Huang, J. Shen, A novel glucose biosensor based on phosphonic acid-functionalized silica nanoparticles for sensitive detection of glucose in real samples, Electrochim. Acta 89 (2013) 278–283.
[3] B. Unnikrishnan, S. Palanisamy, S.M. Chen, A simple electrochemical approach to fabricate a glucose biosensor based on graphene–glucose oxidase biocomposite, Biosens. Bioelectron. 39 (2013) 70–75.
[4] P. Si, P. Kannan, L.H. Guo, H.S. Son, D.H. Kim, Highly stable and sensitive glucose biosensor based on covalently assembled high density Au nanostructures, Biosens. Bioelectron. 26 (2011) 3845–3851.
[5] C.Y. Deng, J.H. Chen, Z. Nie, S.H. Si, A sensitive and stable biosensor based on the direct electrochemistry of glucose oxidase assembled layer-by-layer at the multiwall carbon nanotube-modified electrode, Biosens. Bioelectron. 26 (2010) 213–219.
[6] C.S. Shan, H.F. Yang, J.F. Song, D.X. Han, A. Ivaska, L. Niu, Direct electrochemistry of glucose oxidase and biosensing for glucose based on graphene, Anal. Chem. 81 (2009) 2378–2382.
[7] M. Baghayeri, E.N. Zare, M.M. Lakouraj, Novel superparamagnetic PFu@Fe_3O_4 conductive nanocomposite as a suitable host for hemoglobin immobilization, Sensors Actuators B 202 (2014) 1200–1208.

[8] M. Baghayeri, E.N. Zare, M.M. Lakouraj, A simple hydrogen peroxide biosensor based on a novel electro-magnetic poly(p-phenylenediamine)@Fe_3O_4 nanocomposite, Biosens. Bioelectron. 55 (2014) 259–265.
[9] M. Baghayeri, M. Namadchian, Fabrication of a nanostructured luteolin biosensor for simultaneous determination of levodopa in the presence of acetaminophen and tyramine: application to the analysis of some real samples, Electrochim. Acta 108 (2014) 22–31.
[10] M. Baghayeri, E.N. Zare, R. Hasanzadeh, Facile synthesis of PSMA-g-3ABA/MWCNTs nanocomposite as a substrate for hemoglobin immobilization: application to catalysis of H_2O_2, Mater. Sci. Eng. C 39 (2014) 213–220.
[11] M. Baghayeri, H. Veisi, H. Veisi, B. Maleki, H.K. Maleh, H. Beitollahi, Multi-walled carbon nanotubes decorated with palladium nanoparticles as a novel platform for electrocatalytic sensing applications, RSC Adv. 4 (2014) 49595–49604.
[12] A.A. Saei, P.N. Marandi, A. Abhari, M.D.L. Guardia, J.E.N. Dolatabadi, Electrochemical biosensors for glucose based on metal nanoparticles, Trends Anal. Chem. 42 (2013) 216–227.
[13] F. Caruso, Hollow inorganic capsules via colloid-templated layer-by-layer electrostatic assembly, Top. Curr. Chem. 227 (2003) 145–168.
[14] F. Caruso, Nanoengineering of particle surface, Adv. Mater. 13 (2001) 11–22.
[15] D.Y. Wang, A.L. Rogach, F. Caruso, Semiconductor quantum dot-labeled microsphere bioconjugates prepared by stepwise self-assembly, Nano Lett. 2 (2002) 857–861.
[16] H. Hosseini, M. Behbahani, M. Mahyari, H. Kazerooni, A. Bagheri, A. Shaabani, Ordered carbohydrate-derived porous carbons immobilized gold nanoparticles as new electrode material for electrocatalytical oxidation and determination of nicotinamide adenine dinucleotide, Biosens. Bioelectron. 59 (2014) 412–417.
[17] M. Mahyari, A. Shaabani, M. Behbahani, A. Bagheri, Thiol-functionalized fructose-derived nanoporous carbon as a support for gold nanoparticles and its application for aerobic oxidation of alcohols in water, Appl. Organomet. Chem. 28 (2014) 576–583.
[18] R.G. Chaudhuri, S. Paria, Core/shell nanoparticles: classes, properties, synthesis mechanisms, characterization, and applications, Chem. Rev. 112 (2012) 2373–2433.
[19] S. Karele, S.W. Gosavi, J. Urban, S.K. Kularni, Nanoshell particles: synthesis, properties and applications, Curr. Sci. 91 (2006) 1038–1052.
[20] S.J. Oldenberg, R.D. Averitt, S.L. Westcott, N.J. Halas, Nanoengineering of optical resonances, Chem. Phys. Lett. 288 (1998) 243–247.
[21] F.X. Liu, Z.S. Cao, C.J. Tang, L. Chen, Z.L. Wang, Ultrathin diamond-like carbon film coated silver nanoparticles-based substrates for surface-enhanced Raman spectroscopy, ACS Nano 4 (2010) 2643–2648.
[22] J.X. Zhu, T. Sun, H.H. Hng, J. Ma, F.Y.C. Boey, X.W. Lou, H. Zhang, C. Xue, H.Y. Chen, Q.Y. Yan, Fabrication of core–shell structure of M@C (M = Se, Au, Ag_2Se) and transformation to yolk–shell structure by electron beam irradiation or vacuum annealing, Chem. Mater. 21 (2009) 3848–3852.
[23] Y.G. Wang, Y.R. Wang, E. Hosono, K.X. Wang, H.S. Zhou, The design of a $LiFePO_4$/Carbon nanocomposite with a core–shell structure and its synthesis by an in situ polymerization restriction method, Angew. Chem. Int. Ed. 47 (2008) 7461–7465.
[24] X.M. Sun, Y.D. Li, Ag@C core/shell structured nanoparticles: controlled synthesis, characterization, and assembly, Langmuir 21 (2005) 6019–6024.
[25] X.M. Sun, Y.D. Li, Colloidal carbon spheres and their core/shell structures with noble-metal nanoparticles, Angew. Chem. Int. Ed. 43 (2004) 597–601.
[26] L. Li, J. Sun, X.R. Li, Y. Zhang, Z.X. Wang, C.R. Wang, J.W. Dai, Q.B. Wang, Controllable synthesis of monodispersed silver nanoparticles as standards for quantitative assessment of their cytotoxicity, Biomaterials 33 (2012) 1714–1721.
[27] M. Rycenga, C.M. Cobley, J. Zeng, W.Y. Li, C.H. Moran, Q. Zhang, D. Qin, Y.N. Xia, Controlling the synthesis and assembly of silver nanostructures for plasmonic applications, Chem. Rev. 111 (2011) 3669–3712.
[28] D.V. Goia, E. Matijević, Preparation of monodispersed metal particles, New J. Chem. 22 (1998) 1203–1215.
[29] Q. Fan, D. Shan, H.G. Xue, Y.Y. He, S. Cosnier, Amperometric phenol biosensor based on laponite clay–chitosan nanocomposite matrix, Biosens. Bioelectron. 22 (2007) 816–821.
[30] P. Ye, Z.K. Xu, J. Wu, C. Innocent, P. Seta, Nanofibrous poly(acrylonitrile-*co*-maleic acid) membranes functionalized with gelatin and chitosan for lipase immobilization, Biomaterials 27 (2006) 4169–4176.
[31] X.H. Kang, J. Wang, H. Wu, I.A. Aksay, J. Liu, Y.H. Lin, Glucose Oxidase–graphene–chitosan modified electrode for direct electrochemistry and glucose sensing, Biosens. Bioelectron. 25 (2009) 901–905.
[32] S.Q. Liu, H.X. Ju, Reagentless glucose biosensor based on direct electron transfer of glucose oxidase immobilized on colloidal gold modified carbon paste electrode, Biosens. Bioelectron. 19 (2003) 177–183.
[33] E. Laviron, General expression of the linear potential sweep voltammogram in the case of diffusionless electrochemical systems, J. Electroanal. Chem. 101 (1979) 19–28.
[34] S.Y. Deng, G.Q. Jian, J.P. Lei, Z. Hu, H.X. Ju, A glucose biosensor based on direct electrochemistry of glucose oxidase immobilized on nitrogen-doped carbon nanotubes, Biosens. Bioelectron. 25 (2009) 373–377.
[35] F. Lia, C.S. Shan, F.H. Li, L. Niu, Carbon nanotube/gold nanoparticles/polyethylenimine-functionalized ionic liquid thin film composites for glucose biosensing, Biosens. Bioelectron. 24 (2008) 945–950.
[36] R.A. Kamin, G.S. Wilson, Rotating ring-disk enzyme electrode for biocatalysis kinetic studies and characterization of the immobilized enzyme layer, Anal. Chem. 52 (1980) 1198–1205.
[37] Z.J. Yang, Y. Tang, J. Li, Y.C. Zhang, X.Y. Hu, Facile synthesis of tetragonal columnar-shaped TiO_2 nanorods for the construction of sensitive electrochemical glucose biosensor, Biosens. Bioelectron. 54 (2014) 528–533.
[38] M. Cui, B. Xu, C.G. Hu, H.B. Shao, L.T. Qu, Direct electrochemistry and electrocatalysis of glucose oxidase on three-dimensional interpenetrating, porous grapheme modified electrode, Electrochim. Acta 98 (2013) 48–53.
[39] A. Salimi, A. Noorbakhsh, Layer by layer assembly of glucose oxidase and thiourea onto glassy carbon electrode: fabrication of glucose biosensor, Electrochim. Acta 56 (2011) 6097–6105.
[40] S. Palanisamy, C. Karuppiah, S.M. Chen, Direct electrochemistry and electrocatalysis of glucose oxidase immobilized on reduced graphene oxide and silver nanoparticles nanocomposite modified electrode, Colloids Surf. B: Biointerfaces 114 (2014) 164–169.
[41] Z.H. Yang, X.C. Huang, R.C. Zhang, J. Li, Q. Xu, X.Y. Hu, Novel urchin-like In_2O_3-chitosan modified electrode for direct electrochemistry of glucose oxidase and biosensing, Electrochim. Acta 70 (2012) 325–330.
[42] C.L. Fu, W.S. Yang, X. Chen, D.G. Evans, Direct electrochemistry of glucose oxidase on a graphite nanosheet–Nafion composite film modified electrode, Electrochem. Commun. 11 (2009) 997–1000.
[43] K. Wang, Q. Liu, Q.M. Guan, J. Wu, H.N. Li, J.J. Yan, Enhanced direct electrochemistry of glucose oxidase and biosensing for glucose via synergy effect of grapheme and CdS nanocrystals, Biosens. Bioelectron. 26 (2011) 2252–2257.